DMD Fast Forward. Published on December 15, 2006 as doi:10.1124/dmd.106.012401

Cross-Species Pharmacokinetic Comparison from Mouse to Man of a Second Generation Antisense Oligonucleotide ISIS 301012, Targeting Human ApoB-100

Authors

Rosie Z. Yu, Tae-Won Kim, An Hong, Tanya A. Watanabe, Hans J. Gaus, and Richard S. Geary

Primary laboratory of origin:

Isis Pharmaceuticals, Inc.

Affiliations:

Isis Pharmaceuticals, Inc., RZY, TWK, AH, TW, HG, RSG

DMD Fast Forward. Published on December 15, 2006 as DOI: 10.1124/dmd.106.012401
This article has not been copyedited and formatted. The final version may differ from this version.

Running Title: Cross-Species Pharmacokinetics of a Second Generation Antisense Oligonucleotide

Corresponding Author

Rosie Z. Yu, Ph.D.

Isis Pharmaceuticals, Inc.

1896 Rutherford Road

Carlsbad, CA 92008

Tel: 760 603-2549

Fax: 760 603-3862

Email: ryu@isisph.com

Number of text pages: **39**

Number of tables: **5**

Number of figures: **8**

Number of references: **43**

Number of words in the abstract: **262**

Number of words in the introduction: **624**

Number of words in the discussion: **842**

DMD Fast Forward. Published on December 15, 2006 as DOI: 10.1124/dmd.106.012401
This article has not been copyedited and formatted. The final version may differ from this version.

LIST OF ABBREVIATIONS

ASO	Antisense oligonucleotides
ApoB-100	Apolipoprotein B-100
VLDL-C	Very low density lipoprotein cholesterol
IDL-C	Intermediate density lipoprotein cholesterol
LDL-C	Low-density lipoprotein cholesterol
IACUC	Institutional Animal Care and Use Committee
QWBA	Quantitative whole-body autoradioluminography
ELISA	Enzyme-linked immunosorbent assay
LLOQ	The lower limit of quantitation
CGE	Capillary gel electrophoresis
LSC	Liquid scintillation counting
SPE	Solid phase extraction
HPLC	High performance liquid chromatography
ES/MS	Electrospray mass spectrometry
TIC	Total ion current

ABSTRACT

The pharmacokinetics of a 2'-O-(2-methoxyethyl) modified oligonucleotide, ISIS 301012 (targeting human apoB-100), was characterized in mouse, rat, monkey, and man. Plasma pharmacokinetics following parental administration was similar across species, exhibiting a rapid distribution phase with $t_{1/2\alpha}$ of several hour(s) and a prolonged elimination phase with $t_{1/2\beta}$ in days. The prolonged elimination phase represents equilibrium between tissues and circulating drug due to slow elimination from tissues. Absorption was nearly complete following s.c. injection, with bioavailability ranging from 80% to 100% in monkeys. Plasma clearance scaled well across species as a function of body weight alone, and this correlation was improved when corrected for plasma protein binding. In all animal models studied, the highest tissue concentrations of ISIS 301012 were observed in kidney and liver. Urinary excretion was less than 3% in monkeys and man in the first 24 hours. ISIS 301012 is highly bound to plasma proteins, likely preventing rapid removal by renal filtration. However, following 25 mg/kg s.c. administration in mouse and 5 mg/kg i.v. bolus administration in rat, plasma concentrations of ISIS 301012 exceeded their respective protein binding capacity. Thus, urinary excretion increased to 16% or greater within the first 24 hours. Albeit slow, urinary excretion of ISIS 301012 and its shortened metabolites is the ultimate elimination pathway of this compound, as demonstrated by 32% of dose recovered in total excreta by 14 days in a rat mass balance study. The pharmacokinetics of ISIS 301012 in man is predictable from the pharmacokinetics measured in animals. The pharmacokinetic properties of ISIS 301012 provide guidance for clinical development and support infrequent dose administration.

INTRODUCTION

There have been continued advancements towards identification of chemical modifications that improve upon the pharmacokinetic and pharmacodynamic properties of antisense oligonucleotides (ASOs) over the years (Wagner, 1994; Altmann et al., 1996; Lima et al., 1997; Manoharan, 1999). Amongst the vast majority of these modified phosphorothioate (PS) oligonucleotides, the 2'-O-methoxyethyl (2'-MOE) modified PS oligodeoxynucleotides have consistently demonstrated greater biological stability, higher binding affinity to its target mRNA while maintaining RNase H activity by using a chimeric design strategy (Manoharan, 1999) and decreasing general non-hybridization toxicities (McKay et al., 1999; Henry et al., 2001). These modifications are commonly known as second generation ASOs. Several MOE modified oligonucleotides are in clinical development, including ISIS 104838 for the treatment of rheumatoid arthritis (Sewell et al., 2002; Wei et al., 2003), ISIS 113715 for the treatment of diabetes (Kjems, 2005), OGX-011 for the treatment of prostate cancer (Chi et al., 2004), and LY2181308 for the treatment of solid tumors (Jones and Schreiber, 2005). The MOE modification has led to the development of potent, pharmacologically active, specific antisense oligonucleotides, one of which is ISIS 301012.

ISIS 301012 is a 20-base partially 2'-MOE modified ASO, also referred to as a 5-10-5 MOE gapmer, where the term "gap" refers to the ten 2′-deoxyribonucleosides that are necessary to support enzymatic cleavage of the mRNA (the chimeric design). ISIS 301012 binds to the coding region of the human apoB-100 mRNA (Acc No. NM 000384.1, pos. 3249-3268) by Watson and Crick base-pairing. The hybridization of ISIS 301012 to apoB-100 mRNA results in RNase H-mediated degradation of the cognate mRNA thus inhibiting the translation of the apoB protein. ApoB-100 is the principal apolipoprotein of VLDL-C, IDL-C and LDL-C (Das et al.,

1988; Davidson and Shelness, 2000; Marsh et al., 2002). Thus, apoB-100 inhibition is a promising target for the development of new treatment options to lower LDL-C. ISIS 301012 represents the first antisense compound of the lipid lowering class to be dosed in man (Bradley et al., 2005; Crooke et al., 2005; Kastelein et al, 2006). The in vitro pharmacological activity of ISIS 301012 had been demonstrated in several human cell lines (HepG2 and Hep3B) and primary human hepatocytes, where IC_{50} values were in the range of 10-50 nM for target mRNA reduction.

As expected, there has been significantly more information regarding the pharmacokinetic properties of first-generation PS oligodeoxynucleotides available in the literature since it commenced in the early 1990s (Cossum et al., 1993; Agrawal et al., 1995; Geary et al., 1997b; Leeds et al., 1997; Grindel et al., 1998; Yu et al., 2001a; Yu et al., 2001b) (to cite just a few). Second generation ASOs are relatively early in their development and pharmacokinetic data are less plentiful (Geary et al., 2001a; Sewell et al., 2002; Geary et al., 2003). The pharmacokinetics of ISIS 301012 has been characterized in mice, rats, and monkeys during preclinical development. Additionally, selected pharmacokinetic data in man from a Phase I healthy volunteer study is also included in this manuscript. A compilation of the results of these important studies is described in this manuscript, representing a complete preclinical pharmacokinetic profile for a 2'-O-(2-methoxyethyl) partially-modified antisense phosphorothioate oligonucleotide. Furthermore, the pharmacokinetic analyses used in these studies provide guidance for the development of future oligonucleotide in this chemical class.

METHODS

Test Compound.

ISIS 301012 is a 20-base phosphorothioate oligonucleotide with a total of ten 2'-O-methoxyethyl modified ribofuranosyl nucleotides, five on each end of the oligonucleotide (Figure 1). Full-length purity of the test compound (LC/MS) was 92.8% with 0.5% of the impurities associated with N-1 (deletion sequence). Dosing was performed based on the quantity of full-length 20-mer oligonucleotide.

Radiolabeled ISIS 301012 was mixed together with "cold" ISIS 301012 for radiolabel disposition and mass balance studies in rat. The radiolabel was tritium incorporated in the non-exchangeable 5-carbon position of the ribose sugar of one of the deoxy-thymidine nucleotides in the gap portion of the oligonucleotide (Figure 1). The radiolabel purity of [^{3}H]-ISIS 301012 was >99% by HPLC. The specific activity of [^{3}H]-ISIS 301012 ranged from 20-100 µCi/mg.

Test Systems

Male and female CD-1 mice (Crl:CD-1® (ICR) BR; Charles River Laboratories, Inc., Wilmington, MA), male Sprague-Dawley rats (Crl:CD(SD)IGS BR; Charles River Laboratories Inc., Canada), and male and female cynomolgus monkeys (*Macaca fascicularis;* Sierra Biomedical Animal Colony, Sparks, NV) received either intravenous (i.v.) infusion or subcutaneous (s.c.) injection of ISIS 301012 at doses ranging from 2 to 50 mg/kg. All animal studies were conducted utilizing protocols and methods approved by the Institutional Animal Care and Use Committee (IACUC) and carried out in accordance with the Guide for the Care and Use of Laboratory Animals adopted and promulgated by the U.S. National Institutes of Health.

Mouse

Male and female CD-1 mice were administered ISIS 301012 doses of 2, 5, 25 or 50 mg/kg via s.c. injections every other day for four doses (loading regimen), followed by every fourth day dosing for the duration of a 13-week toxicology study. Drug concentrations were measured in plasma for satellite pharmacokinetic animals receiving the 5 and 25 mg/kg doses. Blood samples were collected for ISIS 301012 quantitation in plasma by cardiac puncture at sacrifice in tubes containing EDTA at 15, 30 and 60 minutes, and 2, 4, 8, 24 and 48 hours following the first dose and the tenth dose (Day 31) (3 male mice per time point). Urine collection over a 48-hour period at 24-hour interval was done immediately following the first dose at the 5 and 25 mg/kg dose levels. Drug concentrations were measured in various types of tissues (including liver and kidney) collected at sacrifice approximately 48 hours after the last dose (Day 93) for all dose groups (2-50 mg/kg). Additionally, concentrations of ISIS 301012 were also measured in tissues of mice receiving the 5 and 50 mg/kg dose sacrificed 91 days after completion of 3-month treatment regimen (on Day 181) to assess clearance during a 3-month recovery phase.

Rat

Single dose i.v. injections of 5 and 24 mg/kg [^{3}H]-ISIS 301012 were administered to male Sprague-Dawley rats. The dose volume was 5 and 6 mL/kg, and the total amount of radioactivity administered was 120 and 1009 µCi/kg, respectively. Prior to dosing, each animal selected for blood collection had a jugular cannula implanted. Following a single i.v. dose of 5 mg/kg [^{3}H]-ISIS 301012, whole blood was collected in tubes containing EDTA at 2, 30 and 60 minutes, and 2, 4, 8, 12, 16, 24 36, 48, 168, 336 and 672 hours post dose from 3 animals/time point. Urinary excretion following the 5 mg/kg dose was assessed at various intervals over a 336-hour period. Mass balance recovery of radiolabel in urine, feces, tissue, carcass and cage

wash was assessed at 24 and 336 hours (or 1 and 14 day after single dose administration 5 mg/kg). Half-lives of total radiolabel were calculated in multiple tissues at a dose of 5 mg/kg (120 µCi/kg) over the 28 days following radiolabeled ISIS 301012 administration. Quantitative whole-body autoradioluminography (QWBA) was performed for rats that received 24 mg/kg (1009 µCi/kg) dose at 48 hours.

Monkey

Single and multiple dose pharmacokinetic studies were conducted in male and female cynomolgus monkeys. Dose levels for ISIS 301012 included 2, 4, and 12 mg/kg administered via 1-hr i.v. infusion; and 20 mg/kg administered by s.c. injection. Doses were administered as every other day for 4 doses (one week), followed by dosing once every fourth day for the remainder of a 13-week dosing period. On Days 7, 27 and 87 (following the 4^{th}, 10^{th} and 24^{th} doses, respectively), blood was collected for quantitation of ISIS 301012 in plasma by peripheral venipuncture into EDTA containing vacutainers just prior to dosing and at 1, 2, 4, 8, 24 and 48 hours following i.v. infusion or s.c. injection. Following the 4^{th} dose of 4 mg/kg ISIS 301012, additional plasma samples were taken 3, 4, 8, 16, 32 and 48 days post dose to assess the terminal elimination half-life in plasma. Urine was collected over a 48-hour period at 24-hour interval immediately following the first dose administration from all dose groups. Drug concentrations were measured in various types of tissues (including liver and kidney) from all dose groups at scheduled terminations (Day 33 and Day 89 sacrifice) and recovery period (Day 181 sacrifice). Accumulation during the loading phase and tissue half-lives were determined in monkeys receiving the 4 mg/kg dose euthanized (1/sex/time point) after a single-dose (48 hours after first dose), or after 4 loading doses (48 hours, and 4, 8, 16, 32, and 48 days after the fourth dose).

Human

In a Phase I clinical study, human healthy volunteers received ISIS 301012 following 2-hr i.v. infusion and s.c. injections at doses that ranged from 50 to 400 mg and has been previously published (Kastelein et al., 2006). Briefly, twenty-nine (29) healthy volunteer subjects in this study received either 50 mg (n = 8), 100 mg (n = 8), 200 mg (n = 9), and 400 mg (n = 4) mg per dose day; seven subjects received placebo. The multiple-dose (MD) period consisted of three i.v. infusions (on MD1, MD3 and MD5) over two hours every other day during the first week, followed by once weekly s.c. injections for 3 weeks (total of 6 doses over 22 days) (on MD8, MD15, and MD22). Intensive pharmacokinetic blood sampling occurred for 24 hours following the first i.v. dose (at 0, 0.5, 1, 2, 2.25, 2.5, 3, 4, 6, 8, and 24 hr), and again following the last s.c. dose (MD22) (at 0, 0.5, 1,1.5, 2, 3, 4, 6, 8, 12 and 24 hr). Additionally, trough blood samples for determination of elimination half-life were collected the post-treatment follow-up period, at 3, 17, 33, 47, 61, 75 and 89 days after the last s.c. dose. Samples were collected in EDTA tubes and plasma was harvested. Urine for pharmacokinetics was collected for the first 24 hours following the first i.v. dose and last s.c. dose. Selected pharmacokinetic data from the Phase I study have been compared to preclinical data and findings summarized.

Analytical Methods

Hybridization ELISA

Plasma samples were analyzed using a quantitative, sensitive hybridization ELISA method which is a variation on the method reported previously (Yu et al., 2002). The assay was validated for precision, accuracy, selectivity, sensitivity and stability of ISIS 301012 quantitation prior to analysis of mouse, monkey and human plasma samples. Plasma sample analyses were

conducted at PPD Development (Richmond, VA) and were performed based on the principles and requirements described in 21 CFR part 58. The assay conducted with synthesized putative shortened oligonucleotide metabolite standards showed no measurable cross-reactivity confirming the assays specificity for the parent oligonucleotide. The lower limit of quantitation (LLOQ) was determined to be 1.52 ng/mL. This assay was also used to quantitate ISIS 301012 concentrations in rat plasma following a single i.v. dose of 5 mg/kg [^{3}H]-ISIS 301012.

Protein Binding Assay

An ultrafiltration method (Watanabe et al., 2006) was used to assess whole plasma protein binding characteristics of ISIS 301012. Briefly, Millipore (Bedford, MA) Ultrafree-MC filters (MW cutoff of 30 K daltons) were used. ISIS 301012 was labeled with ^{32}P prior to addition of the oligonucleotide to plasma (Sambrook et al., 1982). Whole plasma binding of 4 species (mouse, rat, monkey and human) were evaluated over the plasma concentration range of 7.6 to 152 µg/mL. In addition, protein binding in human plasma with selected ISIS 301012 metabolites (N-1 and N-10, or 19-mer and 10-mer) was conducted over the concentration range of 0.1 to 50 µM of ISIS 301012 (equivalent to approximately 0.76 to 380 µg/mL of ISIS 301012). Due to differences in the molecular weight of the ISIS 301012 metabolites, the plasma concentrations were prepared as µM-equivalent concentrations in comparison of length-based plasma protein binding. Five replicates were used to calculate average radiolabel counts and standard deviations.

Capillary Gel Electrophoresis (CGE)

Validated CGE methods were used to measure unlabeled drug concentrations in mouse and monkey urine and tissues, as well as human urine. The methods for ISIS 301012 are

modifications of previously published methods (Leeds et al., 1996; Geary et al., 1999). An internal standard (ISIS 13866, a 27-mer 2'-O-methoxyethyl modified phosphorothioate oligonucleotide) was added prior to extraction. Tissue sample analyses were conducted at Southwest Bio-Labs, inc. (Las Cruces, NM) while urine samples were analyzed at Isis Pharmaceuticals, Inc. Tissue and urine sample analyses were performed based on the principles and requirements described in 21 CFR part 58. For urine and tissues, the limits of quantitation (LOQ) were 0.076 µg/mL, and 1.52 µg/g, respectively.

Radiometric Analysis (LSC)

Radioactivity in rat samples was quantitated by liquid scintillation counting using a Beckman 6001C Counter (Beckman Instruments, Inc, Fullerton, CA). Urine and plasma samples were directly mixed with Ultima Gold LSC cocktail (Packard Instrument Co, Meriden, CT). For solubilized tissue samples, Hionic Fluor LSC cocktail was used (Packard Instrument Co, Meriden, CT). Oxygen combustion of feces and bone was carried out using a Model 307 tissue oxidizer (Packard Instrument Co, Meriden, CT). Ultima Gold cocktail was used to trap the $^{3}H_2O$ generated from each sample. The scintillation counter was operated in the background subtract mode and samples were counted for 5 minutes or to a two-sigma error of 0.1%, whichever occurred first. All counts were converted to absolute radioactivity (dpm) by automatic quench correction based on the shift of the spectrum for the external standard.

Quantitative whole-body autoradioluminography (QWBA)

Rats were sacrificed 48 hours following the 24 mg/kg (200 µCi) i.v. dose administration, and animal carcasses were deep frozen in a mixture of hexane and dry ice. Each animal specimen was then embedded lying on its right side in a 2% carboxymethylcellulose (CMC) medium using

a freezing frame in order to collect sagittal whole-body sections. Each animal specimen block was sectioned using the Leica CM 3600 cryomicrotome. 30 µm sections were collected and were frozen-dry in the microtome cryocabinet for at least 16 hr. Sections were then exposed to ^{3}H-imaging plate for a pre-determined period of time in a lead box and refrigerated at circa 4ºC to minimize background radiation artifacts. Following exposure, the imaging plate was read by the Fuji BAS-2500 scanner and its Fuji Image Reader software version 1.1. From the autoradioluminograms obtained, the amount of radioactivity in tissues was quantified from each animal with reference to calibration curve generated by known ^{3}H-glucose standard radioactivity concentrations using the Fuji Image Gauge Analysis software.

HPLC-ES/MS Metabolite Identification of ISIS 301012 and Metabolites

Selected urine samples from monkey and human were analyzed for metabolite identification purposes by ion pairing (IP) HPLC-ES/MS. Separation was accomplished using an Agilent 1100 HPLC-MS system consisting of a quaternary pump, variable wavelength UV detector, a column oven, an auto sampler and a single quadrupole mass spectrometer MS (Agilent, Wilmington, DE, USA). Typically, 500 µL of each sample was extracted using a 2-step solid phase extraction (SPE) in series (strong anion exchange followed by reverse-phase C18) method, reconstituted in mobile phase and injected directly on a YMC AQ C18 column (150mm x 1.0mm; 3 µm particles; 200 Å pore size, Waters, Milford, MA, USA). The column was maintained at 35 ºC and flow rate on the column was 0.1 mL/min. The column was equilibrated with 35 % acetonitrile in 5mM tributylammonium acetate, pH 7.0. A gradient from 35 to 75% acetonitrile over 27 minutes was used to separately elute ISIS 301012 and shortened oligonucleotide metabolites. Absorbance was measured at 260 nm. Under these conditions, oligonucleotides differing by a single nucleotide could be resolved.

Mass measurements were made on-line using an Agilent single quadrupole mass spectrometer. From 4 to 30 minutes, the mass spectrometer was set to scan a *m/z* window of 800 to 1920. Mass spectra were obtained using a spray voltage of 4 kV, a sheath gas flow of 35 psig, a drying gas flow rate of 12 L/min at 335 ºC and a capillary voltage of –150 V. Chromatograms were analyzed using Agilent Chemstation software. Potential metabolite peaks were identified either from the total ion current (TIC) trace, or from the UV trace. Each peak was manually averaged for its *m/z* value, and the results were compared to a table containing the calculated *m/z* values of expected metabolites.

Pharmacokinetic Analysis

Both compartmental and noncompartmental analysis methods were used for pharmacokinetic characterization of the plasma concentration data (WinNonlin 4.0, Pharsight Corporation, Mountainview, CA). Plasma bioavailability (F) following subcutaneous administration relative to i.v. administration in monkey and man was calculated by the ratio of the dose normalized plasma AUCs.

Cross-species regression utilizing allometry was performed by linear regression of plasma clearance (CL_p) vs. body weight (W). The equation used to relate the pharmacokinetic parameters (Y) to body weight (W) was as follows:

$$Y = aW^b$$

In addition, correction on clearance was made for plasma protein binding, where the unbound intrinsic clearance (CL_u) was calculated by:

$$CL_u = CL_p/f_u$$

Where, f_u is unbound fraction of ISIS 301012 in plasma.

Thus, a log-log regression of a pharmacokinetic parameter, Y (i.e., CL_p or CL_u), versus body weight (W) will yield a y-intercept value of *a* and a slope of b. The sign and magnitude of the exponent (b) indicates how the physiological variable is changing as a function of body weight (W) (Boxenbaum, 1982). Clearance estimates were adjusted by mean body weight for mouse, rat, monkeys, and humans.

First-order elimination rates for ISIS 301012 in tissue were calculated using non-compartmental nonlinear regression of the decay curves for the respective tissues. Half-life was calculated by dividing 0.693 by the first-order elimination rate.

RESULTS

Plasma Pharmacokinetics

The plasma concentration-time profile decreased rapidly in a polyphasic manner for mouse, rat, monkey and human following s.c., i.v. bolus, 1- or 2-hr i.v. administration (Table 1, Figures 2a and 2b). The initial distribution half-life ($t_{1/2\alpha}$) following i.v. bolus administration was relatively fast, generally $\leq$ 1 hour. In monkeys, mean absolute plasma bioavailability (F) after s.c. dosing was 82.8% (Table 2), which would appear to indicate nearly complete systemic absorption by this route of administration. Comparison of tissue levels following s.c. dosing indicates essentially equivalent levels of oligonucleotide in tissues of distribution again indicating essentially complete absorption by the route of administration.

Use of an ultra-sensitive hybridization ELISA method provided characterization of a slow terminal elimination phase in rat, monkey and man (Figure 2b), with a half-life that ranged from 4.7 to 31 days (Table 1). The ISIS 301012 concentration decline in plasma slowed dramatically after nearly complete distribution, which is reflected by a 2 to 4 log decline of ISIS 301012

concentrations in plasma over a period of approximately 24 hours. The apparent terminal elimination rate in monkey plasma, with a half-life of approximately 16 days, was consistent with the slow elimination of ISIS 301012 from monkey tissues, and thus, appears to reflect equilibrium with oligonucleotide in tissue. The terminal elimination phase observed in man was similar to that observed in monkeys (Figure 2b) at a similar mg/kg dose. Consistent with extensive distribution and the long elimination half-lives, the volume of distribution at steady-state was large. For example, the volume of distribution was 7.7 liters/kg in the monkeys and was 48.3 liters/kg in man consistent with extensive distribution of ISIS 301012.

Allometric comparison of clearance estimated at doses ranging from 4 to 5 mg/kg across all species from mouse to man shows a linear relationship (b= 0.65, r^2= 0.95) based on body weight alone (Figure 3a). This correlation improved when clearance was corrected by plasma protein binding (unbound intrinsic clearance, CLu) (b= 0.75, r^2= 0.97) (Figure 3b).

Protein Binding

The percent of ISIS 301012 bound to plasma proteins was ≥85% across the concentration range tested (7.6 – 152 µg/mL) in all species (Figure 4a). The plasma binding extent was highest in human, and lowest in mouse among the species studied. The lower plasma protein binding extent in mouse could partially explain its more rapid clearance. Therefore, allometric scaling of clearance across species corrected by plasma protein binding improved the correlation (Figure 3b). Plasma protein binding appears to be length-dependent, as shorter metabolites (N-1 and N-10) were less plasma protein bound, with the free fraction of N-10 increased 2 to 3-fold compared to ISIS 301012 in human plasma (Figure 4b).

Tissue Distribution and Pharmacokinetics

Tissue distribution in mouse, rat, and monkey (Figures 5 and 6) was similar, wherein the highest concentrations of oligonucleotides were found in kidney and liver. While highest concentrations were seen in liver of mice, the highest concentrations in rat and monkey were observed in kidney. Slightly lower concentrations were detected in lymph nodes, spleen, and bone marrow. The concentrations found in heart, lung, ovaries, uterus, and testes were much lower, with no distribution to brain. Tissue concentrations of ISIS 301012 were generally higher in monkeys than in mice at comparable dose levels (Figure 5).

Following a 20 mg/kg s.c. injection of ISIS 301012 in monkeys, the bioavailability in tissue exposure was nearly 100% (Table 2). The high tissue concentrations suggests that there was complete absorption from the subcutaneous injection site with oligonucleotide reaching tissues in a pattern and at levels similar to intravenous administration, consistent with plasma pharmacokinetics.

Clearance of ISIS 301012 from tissues is dependent on metabolism and was slow compared to the initial plasma clearance. Tissue elimination half-lives for ISIS 301012 were similar across species and were ≥13 days in rats compared to 18 to 35 days in monkeys depending on tissue (Table 3). In addition, tissue clearance was monitored in mice and monkeys during the recovery phase of the toxicology studies. Concentrations of ISIS 301012 decreased approximately 2- to 44-fold in mouse tissues and 4- to 6-fold in monkey tissues after three months of treatment-free recovery period (Day 181) (internal report).

Excretion

Urinary excretion of total oligonucleotide, within the first 24-hours after a single dose, accounted for only a small percentage of the administered dose in mouse, rat and monkey (Table 4). In

general, the percentage of urinary excretion appeared to be dose-dependent as studied in mouse, monkey and man. Urinary excretion in mouse increased with increasing dose, with approximately 1.05% and 23.7% of the dose recovered in urine 24 hours after a single dose of 5 and 25 mg/kg, respectively. The dose dependence of ISIS 301012 excretion in mouse is most likely due to increasing concentrations of unbound drug at higher plasma drug concentrations, which was reflected in its lower plasma protein binding extent. Consistent with this but to a lesser extent, the dose-dependent urinary excretion of ISIS 301012 was observed in monkey and human. The dose-dependent differences are less in monkey and human likely due to greater plasma protein binding extent (Figure 4b) as compared to mice. The majority of urinary excretion occurred within the first 24 hours following dose administration, and decreased dramatically in the next 24-hour period (24-48 hours collection) (data not shown). This biphasic urinary excretion represents a greater extent of excretion when plasma concentrations are higher (early in the plasma profile) likely once again associated with higher levels of unbound drug. Following i.v. bolus administration of 5 mg/kg [^{3}H]-radiolabeled ISIS 301012 in rats, the percentage of total radiolabel dose excreted in urine was approximately 16% over the first 24 hours (Table 4). Albeit slow, urinary excretion is a continuous process, as presented in Figure 7. Approximately 26% of the ISIS 301012-associated radiolabel in rats was excreted by 2 weeks after a single dose. Fecal excretion accounted for less than 5% of the administered dose over the same 2-week period following a single i.v. dose in rats. Urinary and fecal excretion are minor contributors to initial plasma clearance of drug with less than 20% excreted in urine and 5% in feces in 24 hours. However, urinary excretion was the major route of whole body clearance with continuous albeit slow excretion of parent oligonucleotide and nuclease-generated metabolites. The mean mass balance of radioactivity recovered was approximately 83% of the

administered dose at the 24 and 336 hour time points. The majority of radioactivity (approximately 51%) was associated with the tissues (including carcass) and approximately 32% was associated with total excreta and the gastro-intestinal tract contents (26% in urine, 4.2% in feces, 0.99% in cage wash, and 0.44% in the gastro-intestinal tract contents) after two weeks (336 hours). These findings appeared to be consistent with relatively rapid and almost complete distribution of [^{3}H]-ISIS 301012-related radioactive residues from the blood to tissues following intravenous administration, followed by relatively slow clearance of the radiolabeled species from tissues into the excreta (mainly urine).

In monkey and human, urinary excretion of total oligonucleotide within the first 24 hours, accounted for only a small percentage of the administered dose (mean excretion less than 4% of administered dose) following a single dose up to 12 mg/kg in monkey and 200 mg in human given by 1- or 2-hour infusion (Table 4). In addition to parent compound, putative oligonucleotide metabolites consistent with mainly endonuclease-mediated cleavage were evident in most of the collected urine samples in monkey and human (Figure 8). However, ISIS 301012 was typically the most abundant species of oligonucleotides and generally accounted for >60% of the total oligonucleotide in the urine samples.

Urinary Metabolite Identification

Numerous ISIS 301012 metabolites were detected in urine collected 0-24 hr following dose administration in monkey and human. These metabolites were characterized using a sensitive IP-HPLC-ES/MS method and confirmed the identity of these shorter oligonucleotides in urine (Table 5), consistent with mainly endonuclease-mediated metabolism. In fact, the IP-HPLC provided baseline resolution for a majority of the metabolites, with nucleotide length of 7 to 14

nucleotides (Figure 8). In tissues analyzed by CGE, the same metabolites were detected suggesting that these metabolites are generated in tissues and subsequently excreted in urine.

DISCUSSION

Plasma pharmacokinetics of the of 2'-MOE partially modified ISIS 301012 were similar in mice, rats, monkeys and humans in that drug was cleared from plasma rapidly and distributed to tissues. This pharmacokinetic behavior has been observed for unmodified phosphorothioate oligodeoxynucleotides (first generation oligodeoxynucleotides) as well as other 2'-MOE partially modified oligodeoxynucleotides of the same chemical class as ISIS 30102 but of different sequence (Geary et al., 1997a; Geary et al., 2003). Following parenteral administration, plasma concentration-time profiles of ISIS 301012 are poly-phasic, characterized by a rapid distribution phase (half-lives in hours), followed by at least one additional much slower elimination phase with half-lives from 5-31 days. The recent development of ultra-sensitive hybridization ELISA methods have made it possible to characterize plasma concentrations up to 3 months after dose administration, enabling the determination of terminal plasma elimination half-lives (Yu et al., 2001c; Sewell et al., 2002; Yu et al., 2002; Geary et al., 2003). Most importantly, the plasma concentrations of ISIS 301012 observed in the terminal elimination phase represent ISIS 301012 that is in equilibrium with tissue(s) and thus provide a measure of tissue elimination rate (based on nonclinical experience with measured tissue elimination over time).

Allometric analysis of plasma pharmacokinetics for multiple antisense phosphorothioate oligonucleotides (ASOs) from mouse to man confirm the predictability of the pharmacokinetics across species and the ability to extrapolate exposure directly on a mg/kg basis (Geary et al., 1997a; Geary et al., 2001b; Geary et al., 2003). These relationships are once again demonstrated

with ISIS 301012 data, where plasma clearance and unbound intrinsic clearance scaled well across species using body weight.

The majority of drug was removed from plasma by distribution to tissues within the first 24 hours following drug administration. The low abundance of the shortened metabolites in tissue is consistent with the long tissue elimination half-life of this compound and short half-life of the metabolites. Relative to plasma distribution (half-life in minutes to hours), tissue elimination was slow (half-life in days). ISIS 301012 in tissue was cleared slowly over the course of weeks, and tissue half-lives are approximately 5-fold longer than for first generation ASOs (Agrawal et al., 1995; Phillips et al., 1997; Geary et al., 2001c; Yu et al., 2001a; Geary et al., 2003; Yu et al., 2004). The slow clearance from tissues allowed for maintenance of tissue concentrations with relatively infrequent dosing. Nevertheless, care must be taken in the interpretation of the terminal elimination rate since it is, by definition, a composite of multiple tissues with the slowest eliminating tissue ultimately dominating the composite plasma elimination rate. The observed organ to organ differences in ISIS 301012 clearance together with previously described differences in suborgan cellular elimination rates (Yu et al., 2001d), indicate that it is at least possible that the elimination rate described by the terminal plasma phase will overestimate the half-life at the target tissue and/or cell. Ultimately, a combination of clinical testing of multiple dosing frequencies and careful pharmacokinetic/pharmacodynamic analysis should be used to fully characterize the optimal dosing frequency required to ensure continued pharmacological activity at the target.

While distribution to tissues was the mechanism of plasma clearance, whole body clearance is the result of slow metabolism by endo- and exonucleases in tissues, followed by urinary excretion of low molecular weight oligonucleotide metabolites as well as ISIS 301012, and to a

much less extent, fecal excretion of both ISIS 301012 and these metabolites. Ubiquitous endo- and exonucleases are known to metabolize oligonucleotides like ISIS 301012. The endonuclease metabolism results in the formation of oligonucleotide fragments that are the substrates for additional metabolism by exonucleases. The resultant metabolites are shortened oligonucleotides, approximately 8 to 12 nucleotides in length. The metabolites observed in urine are evidence that the earliest cleavage occurs in the 10-base 2'-deoxy gap, effectively splitting the oligomer in half. These data implicate endonuclease digestion as the initial cleavage event. These data are consistent with the nuclease resistance of 2'-MOE modified nucleotides placed in the 3' and 5' terminal portions of ISIS 301012 (Zhang et al., 1995). There was a notable absence of metabolites ranging from 16-19 nucleotides in length suggesting little to no exonuclease products which are often seen with unmodified phosphorothioate oligodeoxynucleotides (Temsamani et al., 1994; Cummins et al., 1996; Gaus et al., 1997). The similarity of the excretion metabolite pattern across species suggests similar enzymes are responsible for metabolic cleavage of oligonucleotides.

The pharmacokinetics of ISIS 301012 in man is predictable from the pharmacokinetics measured in monkeys based on the similarities in plasma pharmacokinetics (C_{max}, AUC and Clearance), and plasma elimination half-life. Because the primary driver for plasma clearance is uptake by tissues, the similarities in the plasma kinetics suggest that there are similarities in distribution as well. Indeed, tissue distribution of ISIS 301012 was similar across species. Like unmodified predecessors, ISIS 301012 is rapidly distributed to tissues but with much longer tissue half-lives. These favorable pharmacokinetic properties for ISIS 301012 provide guidance for clinical development and appear to support infrequent and convenient dose administration.

ACKNOWLEDGEMENTS

The authors wish to thank Dr. Art Levin for scientific discussion and critical review of the manuscript. Finally, this manuscript would not be possible without the administrative support provided by Robert Saunders, for which we are grateful.

REFERENCES

Agrawal S, Temsamani J, Galbraith W and Tang J (1995) Pharmacokinetics of antisense oligonucleotides. Clinical Pharmacokinetics 28:7-16.

Altmann K-H, Dean NM, Fabbro D, Freier SM, Geiger T, Haner R, Husken D, Martin P, Monia BP, Muller M, Natt F, Nicklin P, Phillips J, Pieles U, Sasmor H and Moser H, E. (1996) Second generation of antisense oligonucleotides: From nuclease resistance to biological efficacy in animals. Chimia 50:168-176.

Boxenbaum H (1982) Interspecies scaling, allometry, physiological time, and the ground plan of pharmacokinetics. Journal of Pharmacokinetics and Biopharmaceutics 10:201-227.

Bradley JD, Crooke R, Kjems LL, Graham M, Leong R, Yu R, Paul D and Wedel M (2005) Hypolipidemic effects of a novel inhibitor of human APO-B 100 in humans, in: Diabetes 54(Supplement 1):977-P.

Chi KN, Eisenhauer E, Fazli L, Jones EC, Goldenberg SL, Powers J and Gleave ME (2005) A phase I pharmacokinetic and pharmacodynamic study of OGX-011, a 2'methoxyethyl antisense to clusterin, in patients with localized prostate cancer. Journal of the National Cancer Institute, 97 (17): 1287-1296.

Cossum PA, Sasmor H, Dellinger D, Truong L, Cummins L, Owens SR, Markham PM, Shea JP and Crooke ST (1993) Disposition of the 14C-labeled phosphorothioate oligonucleotide ISIS 2105 after intravenous administration to rats. Journal of Pharmacology and Experimental Therapeutics 267:1181-1190.

Crooke RM, Graham MJ, Lemonidis KM, Whipple CP, Koo S and Perera RJ (2005) An apolipoprotein B antisense oligonucleotide lowers LDL cholesterol in hyperlipidemic mice without causing hepatic steatosis. Journal of Lipid Research 46:872-884.

Cummins LL, Leeds J, Greig M, Griffey RH, Graham MJ, Crooke R and Gaus HJ (1996) Capillary gel electrophoresis and mass spectrometry: Powerful tools for the analysis of antisense oligonucleotides and their metabolites, in: XII International Roundtable, Nucleosides, Nucleotides and their Biological Applications, pp 72, La Jolla, California.

Das HK, Leff T and Breslow JL (1988) Cell type-specific expression of the human apoB gene is controlled by two cis-acting regulatory regions. Journal of Biological Chemistry 263:11452-11458.

Davidson NO and Shelness GS (2000) APOLIPOPROTEIN B: mRNA editing, lipoprotein assembly, and presecretory degradation. Annu Rev Nutr 20:169-193.

Gaus HJ, Owens SR, Winniman M, Cooper S and Cummins LL (1997) On-line HPLC electrospray mass spectrometry of phosphorothioate oligonucleotide metabolites. Analytical Chemistry 69:313-319.

Geary RS, Khatsenko O, Bunker K, Crooke R, Moore M, Burckin T, Truong L, Sasmor H and Levin AA (2001a) Absolute bioavailability of 2'-O-(2-methoxyethyl)-modified antisense oligonucleotides following intraduodenal instillation in rats. Journal of Pharmacology and Experimental Therapeutics 296:898-904.

Geary RS, Leeds JM, Fitchett J, Burckin T, Troung L, Spainhour C, Creek M and Levin AA (1997a) Pharmacokinetics and metabolism in mice of a phosphorothioate oligonucleotide antisense inhibitor of C-raf-1 kinase expression. Drug Metabolism and Disposition 25:1272-1281.

Geary RS, Leeds JM, Henry SP, Monteith DK and Levin AA (1997b) Antisense oligonucleotide inhibitors for the treatment of cancer: 1. Pharmacokinetic properties of phosphorothioate oligodeoxynucleotides. Anti-Cancer Drug Design 12:383-393.

Geary RS, Mathison B, Ushiro-Watanabe T, Savides MC, Henry SP and Levin AA (2001b) Second generation antisense oligonucleotide pharmacokinetics and mass balance following intravenous administration in rats, in: Society Of Toxicology, pp 343, Oxford University Press, San Francisco, CA.

Geary RS, Matson J and Levin AA (1999) A nonradioisotope biomedical assay for intact oligonucleotide and its chain-shortened metabolites used for determination of exposure and elimination half-life of antisense drugs in tissue. Analytical Biochemistry 274:241-248.

Geary RS, Ushiro-Watanabe T, Truong L, Freier SM, Lesnik EA, Sioufi NB, Sasmor H, Manoharan M and Levin AA (2001c) Pharmacokinetic properties of 2'-O-(2-methoxyethyl)-modified oligonucleotide analogs in rats. Journal of Pharmacology and Experimental Therapeutics 296:890-897.

Geary RS, Yu RZ, Watanabe T, Henry SP, Hardee GE, Chappell A, Matson J, Sasmor H, Cummins L and Levin AA (2003) Pharmacokinetics of a tumor necrosis factor-alpha phosphorothioate 2'-O-(2-methoxyethyl) modified antisense oligonucleotide: comparison across species. Drug Metabolism and Disposition 31:1419-1428.

Grindel JM, Musick TJ, Jiang Z, Roskey A and Agrawal S (1998) Pharmacokinetics and metabolism of an oligodeoxynucleotide phosphorothioate (GEM91) in cynomolgus monkeys following intravenous infusion. Antisense and Nucleic Acid Drug Development 8:43-52.

Henry SP, Geary RS, Yu R and Levin AA (2001) Drug properties of second-generation antisense oligonucleotides: how do they measure up to their predecessors? Current Opinion in Investigational Drugs 2:1444-1449.

Jones BA and Schreiber AD (2005) mRNA as a Therapeutic Target in Lung Disease. 2:361-372.

Kastelein JJP, Wedel MK, Baker BF, Su J, Bradley JD, Yu RZ, Chuang E, Graham MJ and Crooke RM (2006) Potent Reduction of Apolipoprotein B and LDL Cholesterol by an Antisense Inhibitor of Apolipoprotein B. Circulation. 114:1729-35.

Kjems L (2005) New Targets for Glycemic Control Protein-Tyrosine-Phosphatase-1B Antisense Inhibitor, in: the American Diabetes Association's 65th Annual Meeting, San Diego, California.

Leeds JM, Geary RS, Henry SP, Glover J, Shanahan W, Fitchett J, Burckin T, Truong L and Levin AA (1997) Pharmacokinetic properties of phosphorothioate oligonucleotides. Nucleosides & Nucleotides 16:1689-1693.

Leeds JM, Graham MJ, Troung L and Cummins LL (1996) Quantitation of phosphorothioate oligonucleotides in human plasma. Analytical Biochemistry 235:36-43.

Lima WF, Venkatraman M and Crooke ST (1997) The influence of antisense oligonucleotide-induced RNA structure on E. coli RNase H1 activity. The Journal of Biological Chemistry 272:18191-18199.

Manoharan M (1999) 2'-carbohydrate modifications in antisense oligonucleotide therapy: importance of conformation, configuration and conjugation. Biochimica et Biophysica Acta 1489:117-130.

Marsh JB, Welty FK, Lichtenstein AH, Lamon-Fava S and Schaefer EJ (2002) Apolipoprotein B metabolism in humans: studies with stable isotope-labeled amino acid precursors. Atherosclerosis 162:227-244.

McKay RA, Miraglia LJ, Cummins LL, Owens SR, Sasmor H and Dean NM (1999) Characterization of a potent and specific class of antisense oligonucleotide inhibitor of human protein kinase C-a expression. Journal of Biological Chemistry 274:1715-1722.

Phillips JA, Craig SJ, Bayley D, Christian RA, Geary RS and Nicklin PL (1997) Pharmacokinetics, metabolism and elimination of a 20-mer phosphorothioate oligodeoxynucleotide (CGP 69846A) after intravenous and subcutaneous administration. Biochemical Pharmacology 54:657-668.

Sambrook J, Maniatis T and Fritsche EF (1982) Molecular cloning: A laboratory manual. Cold Spring Harbor Laboratory Press, Cold Spring Harbor, NY.

Sewell LK, Geary RS, Baker BF, Glover JM, Mant TGK, Yu RZ, Tami JA and Dorr AF (2002) Phase I trial of ISIS 104838, a 2'-methoxyethyl modified antisense oligonucleotide targeting tumor necrosis factor-alpha. Journal of Pharmacology and Experimental Therapeutics 303:1334-1343.

Temsamani J, Kubert M, Tang J, Padmapriya A and Agrawal S (1994) Cellular uptake of oligodeoxynucleotide phosphorothioates and their analogs. Antisense Research and Development 4:35-42.

Wagner RW (1994) Gene inhibition using antisense oligodeoxynucleotides. Nature 372:333-335.

Watanabe TA, Geary RS and Levin AA (2006) Plasma Protein Binding of an Antisense Oligonucleotide Targeting Human ICAM-1 (ISIS 2302). Oligonucleotides 16:169-180.

Wei N, Fiechtner J, Boyle D, Kavanaugh A, Delauter S, Rosengren S, Firestein GS, Tami J, Yu R and Sewell L (2003) Synovial Biomarker Study of ISIS 104838, An Antisense Oligodeoxynucleotide Targeting TNF-alpha, in Rheumatoid Arthritis, in: 67th Annual Meeting of the American College of Rheumatology (ACR), Orlando, Florida.

Yu RZ, Baer B, Chappel A, Geary RS, Chueng E and Levin AA (2002) Development of an ultrasensitive noncompetitive hybridization-ligation enzyme-linked immunosorbent assay for

the determination of phosphorothioate oligodeoxynucleotide in plasma. Analytical Biochemistry 304:19-25.

Yu RZ, Geary RS, Leeds JM, Ushiro-Watanabe T, Moore M, Fitchett J, Matson J, Burckin T, Templin MV and Levin AA (2001a) Comparison of pharmacokinetics and tissue disposition of an antisense phosphorothioate oligonucleotide targeting human Ha-ras mRNA in mouse and monkey. Journal of Pharmaceutical Sciences 90:182-193.

Yu RZ, Geary RS, Monteith DK, Matson J, Truong L, Fitchett J and Levin AA (2004) Tissue disposition of a 2'-O-(2-methoxy) ethyl modified antisense oligonucleotides in monkeys. Journal of Pharmaceutical Sciences 93:48-59.

Yu RZ, Geary RS, Ushiro-Watanabe T, Levin AA and Schoenfeld SL (2001b) Pharmacokinetic properties in humans, in: Antisense Drug Technology: Principles, Strategies, and Applications (Crooke ST ed), pp 183-200, Marcel Dekker, Inc., New York.

Yu RZ, Matson J and Geary RS (2001c) Terminal Elimination Rates for Antisense Oligonucleotides in Plasma Correlate with Tissue Clearance Rates in Mice and Monkeys, AAPS PharmSci Vol. 3, No. 3.

Yu RZ, Zhang H, Geary RS, Graham M, Masarjian L, Lemonidis K, Crooke R, Dean NM and Levin AA (2001d) Pharmacokinetics and pharmacodynamics of an antisense phosphorothioate oligonucleotide targeting Fas mRNA in mice. Journal of Pharmacology and Experimental Therapeutics 296:388-395.

Zhang R, Lu Z, Zhao H, Zhang X, Diasio RB, Habus I, Jiang Z, Iyer RP, Yu D and Agrawal S (1995) In vivo stability, disposition and metabolism of a "hybrid" oligonucleotide phosphorothioate in rats. Biochemical Pharmacology 50:545-556.

Figure Legends

Figure 1. Sequence of ISIS 301012 – fully thioated 20-mer. Bold and underlined nucleotides are 2'-O-(2-methoxyethyl) modified. Center gap, deoxynucleotide (DNA).
Stable tritium [^{3}H] label incorporated on 5' Carbon of an un-modified thymidine residue in ISIS 301012 oligonucleotide.

Figure 2. Polyphasic pharmacokinetic profiles of ISIS 301012 in mouse, rat, monkey and human during distribution (a), and in monkey and man during elimination phase (b). ISIS 301012 concentrations in plasma were measured using a hybridization ELISA method in mouse, rat, monkey and man.

Figure 3. Allometric relationship across species of plasma clearance (CL) with body weight (a) or unbound intrinsic clearance (CLu) with body weight (b). Doses ranged from 4 to 5 mg/kg.

Figure 4. Bound fraction of [^{32}P]-ISIS 301012 to whole plasma protein across species (a) and free fraction of [^{32}P]-labeled ISIS 301012 as well as metabolites in whole human plasma protein (b) as a function of concentration added. Each point represents the mean of 5 measurements, error bar represents standard deviation.

Figure 5. Comparison of ISIS 301012 concentrations in tissues taken 48 hrs after the last dose administered over 3 months to CD-1 mice and cynomolgus monkeys. Each bar represents the average of 3 to 6 measurements (CGE-UV). Error bars are standard deviation.

Figure 6. Distribution of radiolabel associated with [^{3}H]-ISIS 301012 presented by quantitation of radio label by liquid scintillation (µg-eq./mL blood or plasma and µg-eq./g of tissue) in rat 48 hours after single i.v. administration at a dose of 5 mg/kg [^{3}H]-ISIS 301012 (n=3) (a) and by QWBA in male rat, 48 hours after a single intravenous bolus dose of 24 mg/kg [^{3}H]-ISIS 301012 (b). The darkness of the grey scale on the QWBA figure represents the level of radioactivity, where white being the lowest, and black being the highest.

Figure 7. Mass balance excretion of radiolabel residue associated with [^{3}H]-ISIS 301012 over 14 days after single 5 mg/kg i.v. bolus injection in rats.

Figure 8. Representative IP-HPLC chromatogram of urine samples collected at 0-24 hr from monkey and man treated with ISIS 301012.

DMD Fast Forward. Published on December 15, 2006 as DOI: 10.1124/dmd.106.012401
This article has not been copyedited and formatted. The final version may differ from this version.

Table 1. Plasma pharmacokinetic parameter estimates for ISIS 301012 compared across species. Standard deviation of the estimates is shown in parenthesis.

Parameter	Mouse	Rat[a]	Monkey	Human
Dose and route	5 mg/kg s.c.	5 mg/kg i.v. bolus	4 mg/kg 1-hr i.v. infusion	200 mg 2-hr i.v. infusion
C_{max} (µg/ml)	3.8 (0.57)	73.9 (2.4)	39.8 (6.7)	21.5 (4.2)
T_{max} (hour)	0.5	2 min	1 (0)	1.98 (0.21)
AUC (µg*hr/ml)	7.41	27.7	82.0 (19.1)	68.2 (13.5)
$t_{1/2\alpha}$ (hour)	0.33	0.39	0.68 (0.19)	1.26 (0.16)
$t_{1/2\beta}$ (day)	NM	4.7[c]	16[e]	31.1 (11.4)[b]
CL_p (ml/hr/kg)[d]	674	181	51.1 (11.1)	40.9 (5.12)
V_{ss} (L/kg)[d]	NM	1.0	7.7[e]	48.3 (14.7)[b]

[a] ISIS 301012 concentrations were measured using cold assay, hybridization ELISA method.
[b] Determined following s.c. administration
[c], Plasma concentration-time profile appeared tri-phasic, with a half-life of 2.9 hr in the second phase, thus this half-life represents the terminal half-life. Additionally, the terminal half-life may be underestimated because of limited time points.
[d] CLp/F and V_z/F reported for s.c. dosing
[e] N=2

DMD Fast Forward. Published on December 15, 2006 as DOI: 10.1124/dmd.106.012401
This article has not been copyedited and formatted. The final version may differ from this version.

Table 2. Subcutaneous administration of ISIS 301012 to monkeys resulted in essentially complete bioavailability measured by both plasma AUC (Day 7) and tissue concentrations of ISIS 301012 measured 48 hours after the last dose administered over a 13-week period

Parameter	IV	SC	F (%)[a]
Dose	12 mg/kg	20 mg/kg	
Plasma AUC (µg*hr/mL)	310	428	82.8
Kidney Cortex (µg/g)	1304	1593	73.3
Kidney Medulla (µg/g)	684	1221	107
Liver (µg/g)	584	1129	116
Lung (µg/g)	26.9	61.6	137
Mesenteric Lymph (µg/g)	459	767	100
Heart (µg/g)	46.9	93.2	119
Bone Marrow (µg/g)	104	217	125

[a] F (%)= {(Cs.c./Doses.c.) / (Ci.v. /Dosei.v.)} $\times$ 100, where C represents the respective tissue concentration of ISIS 301012 on Day 89.

DMD Fast Forward. Published on December 15, 2006 as DOI: 10.1124/dmd.106.012401
This article has not been copyedited and formatted. The final version may differ from this version.

Table 3. Estimated elimination half-life (in days) of ISIS 301012 from selected tissues in rat and monkey.

Tissue	Rat [b]	Monkey
Dose	**5 mg/kg ^{3}H- ISIS 301012**	**4 mg/kg ISIS 301012**
Kidney [a]	>28	7 [c], 33
Liver	13	34
Mesenteric Lymph node	>28	35
Heart	>28	18

[a] Whole kidney in rat; kidney cortex in monkey

[b] Value is reported as >28 days because the sampling times were collected for 28 days (less than one half-life) and were insufficient to determine elimination half-life. In addition, half-life was estimated from total radioactivity.

[c] Concentration-time profile appears biphasic with a 7 day initial half-life and apparent terminal elimination half-life of 33 days.

Table 4. Fraction of ISIS 301012 dose excreted (%) in urine as ISIS 301012 (parent drug) and its metabolites over the period of 0-24 hours following intravenous and subcutaneous injection at selected doses compared across species.

Parameter	Mouse		Rat[a]	Monkey		Human	
Route	s.c. injection		i.v. bolus	1-hr i.v. infusion		2-hr i.v. infusion	
Dose	5 mg/kg	25 mg/kg	5 mg/kg	2 mg/kg	12 mg/kg	50 mg	200 mg
f_{ex}, ISIS 301012	1.05%	22.2%	NM	0.04%	2.35%	0.91%	1.76%
f_{ex}, metabolites	0%	1.5%	NM	0.22%	0.54%	0.47%	1.54%
f_{ex}, total	1.05%	23.7%	16%	0.26%	2.89%	1.38%	3.30%

f_{ex} = fraction of administered dose excreted in urine

NM = not measured

[a] fraction (%) of total radiolabel dose excreted in urine

DMD Fast Forward. Published on December 15, 2006 as DOI: 10.1124/dmd.106.012401
This article has not been copyedited and formatted. The final version may differ from this version.

Table 5. Tabular summary of LC-ES/MS results for Monkey and Human Urine (0-24 hr collection, monkey dose: 12 mg/kg, human dose: 400 mg).

Name[a]	Length	Sequence	Charge state	m/z	MW expected (Daltons)	MW observed (Daltons)	ΔMS (Daltons)
ISIS 301012	20	GCCTCAGTCTGCTTCGCACC	-4	1793.1	7176.1	7176.4	0.3
A	14	GTCTGCTTCGCACC	-3	1616.8	4853.7	4853.1	-0.6
B	13	TCTGCTTCGCACC	-3	1501.6	4507.7	4508.4	0.7
C	11	TGCTTCGCACC	-3	1288.5	3868.6	3868.2	-0.4
D	10	P(S)-GCTTCGCACC	-3	1208.3	3628.5	3628.8	0.3
E	10	GCTTCGCACC	-3	1181.7	3548.6	3548.4	-0.2
F	10	GCCTCAGTCT	-3	1182.1	3549.6	3549.9	0.3
G	9	GCCTCAGTC	-3	1075.4	3229.5	3228.8	-0.7
H	8	GCCTCAGT	-3	968.9	2909.5	2910	0.5
I	8	TTCGCACC	-3	960.5	2883.5	2883.6	0.1
J	7	GCCTCAG	-2	1293.5	2589.5	2589	-0.5

[a] Refer to Figure 10 for peak identifications.

DMD Fast Forward. Published on December 15, 2006 as DOI: 10.1124/dmd.106.012401
This article has not been copyedited and formatted. The final version may differ from this version.

Figure 1.

5'- GC^{M}C^{M}TC^{M}AGTC^{M}TGC^{M}TTC^{M}GC^{M}AC^{M}C^{M}-3'

C^{M} = 5-methyl cytosine

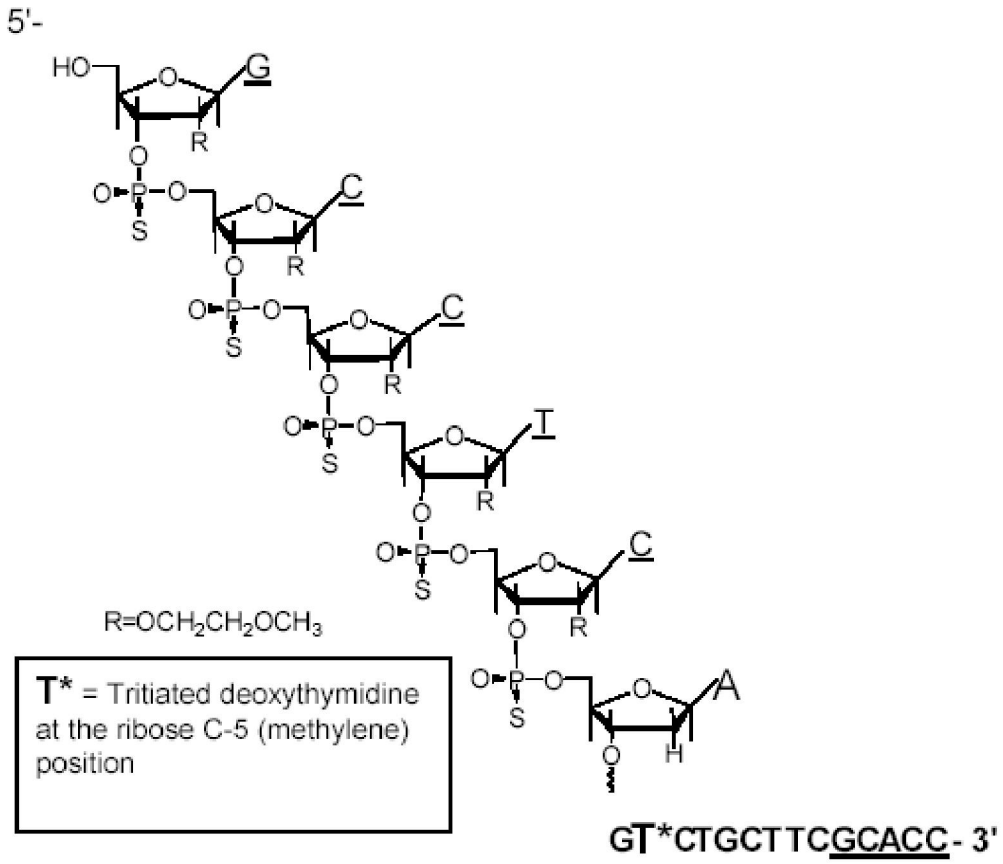

Underlined nucleobases are 2'-O-(2-methoxyethyl) modified.

DMD Fast Forward. Published on December 15, 2006 as DOI: 10.1124/dmd.106.012401
This article has not been copyedited and formatted. The final version may differ from this version.

Figure 2a

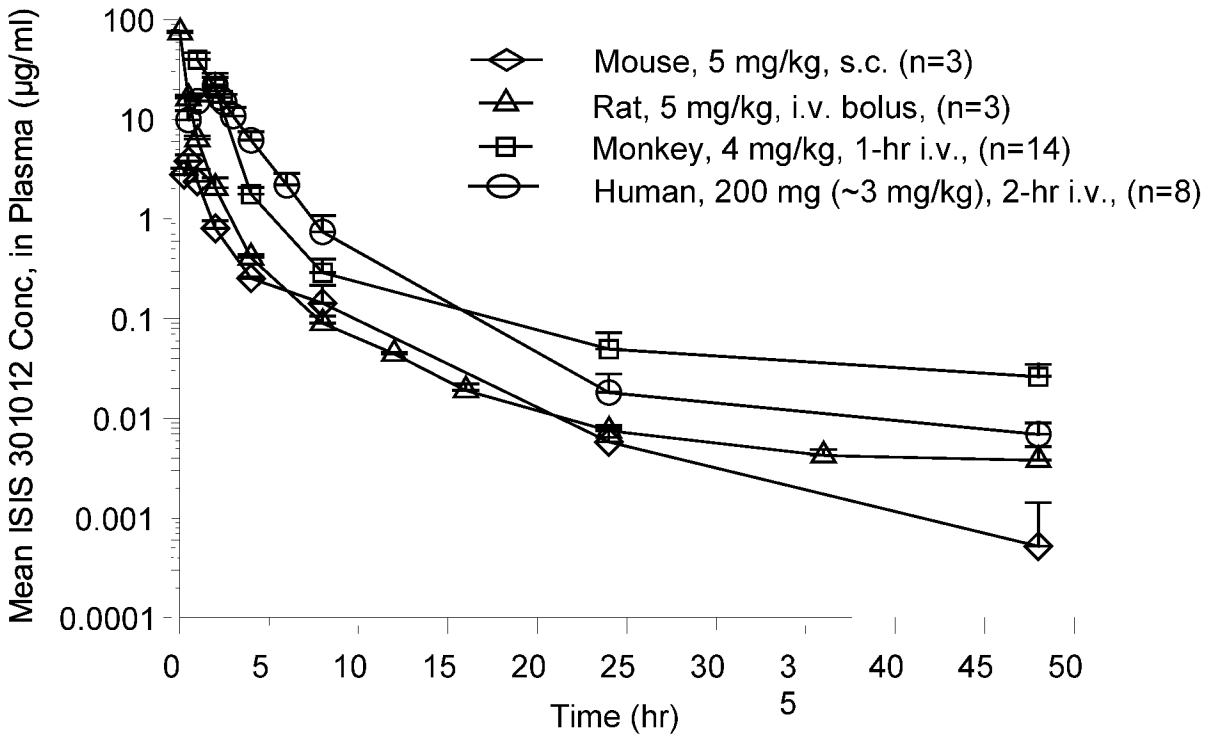

DMD Fast Forward. Published on December 15, 2006 as DOI: 10.1124/dmd.106.012401
This article has not been copyedited and formatted. The final version may differ from this version.

Figure 2b

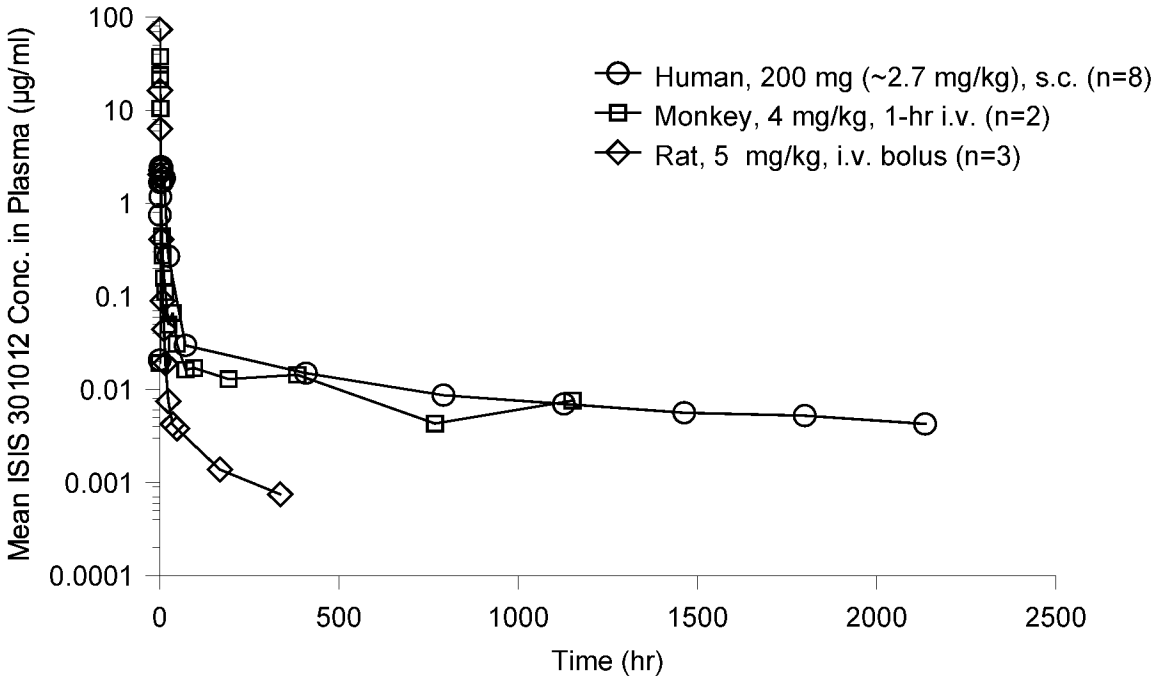

DMD Fast Forward. Published on December 15, 2006 as DOI: 10.1124/dmd.106.012401
This article has not been copyedited and formatted. The final version may differ from this version.

Figure 3a

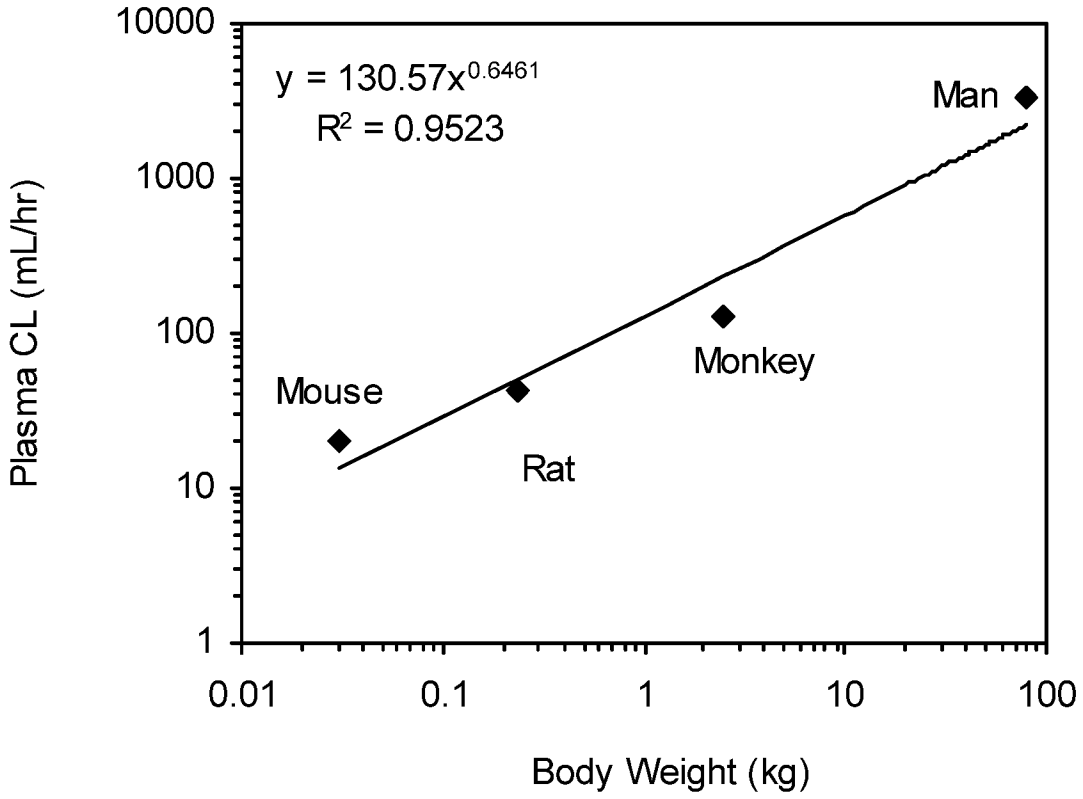

DMD Fast Forward. Published on December 15, 2006 as DOI: 10.1124/dmd.106.012401
This article has not been copyedited and formatted. The final version may differ from this version.

Figure 3b

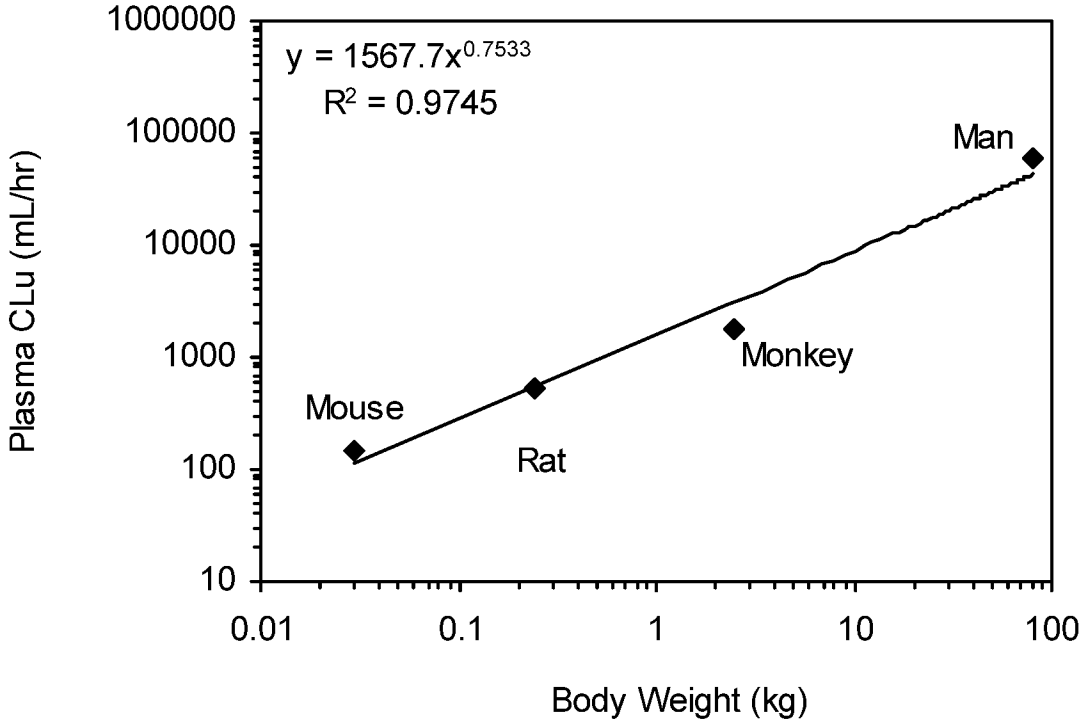

DMD Fast Forward. Published on December 15, 2006 as DOI: 10.1124/dmd.106.012401
This article has not been copyedited and formatted. The final version may differ from this version.

Figure 4a

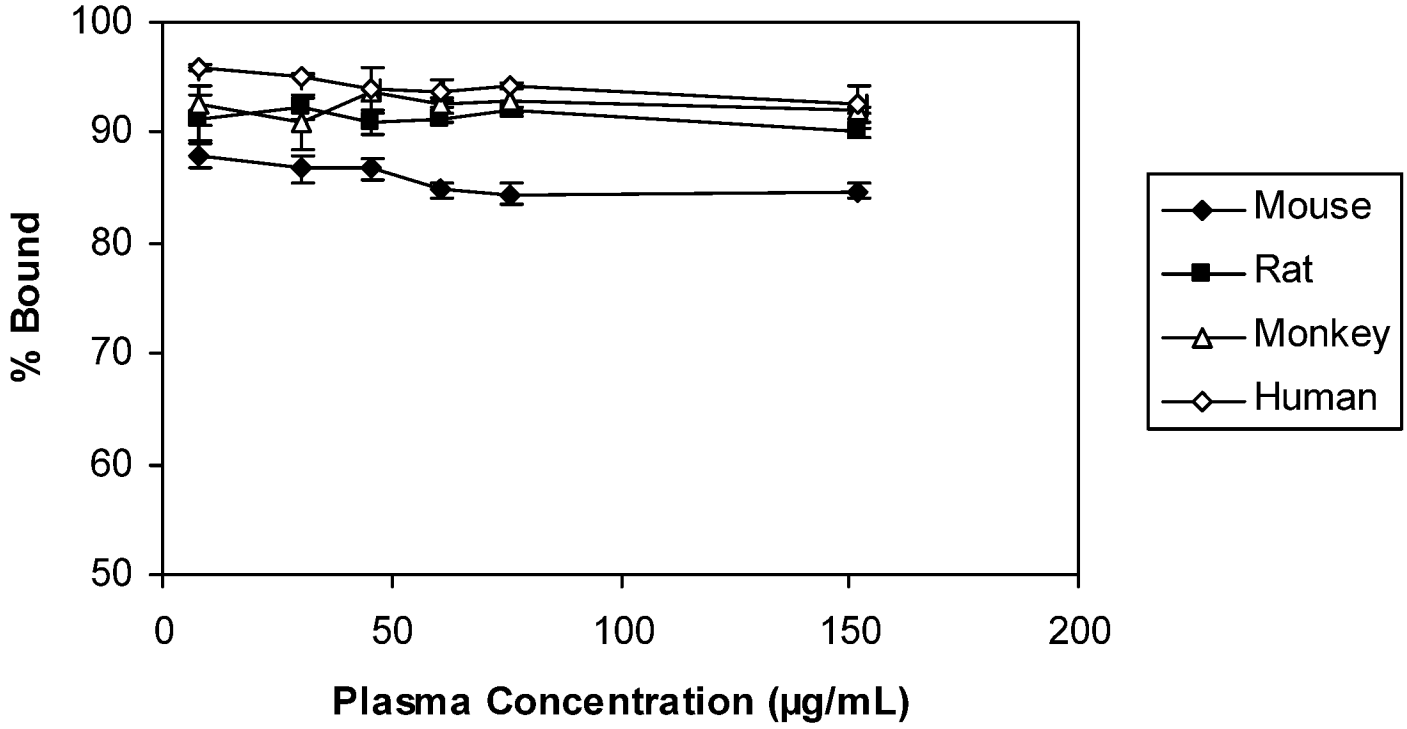

DMD Fast Forward. Published on December 15, 2006 as DOI: 10.1124/dmd.106.012401
This article has not been copyedited and formatted. The final version may differ from this version.

Figure 4b

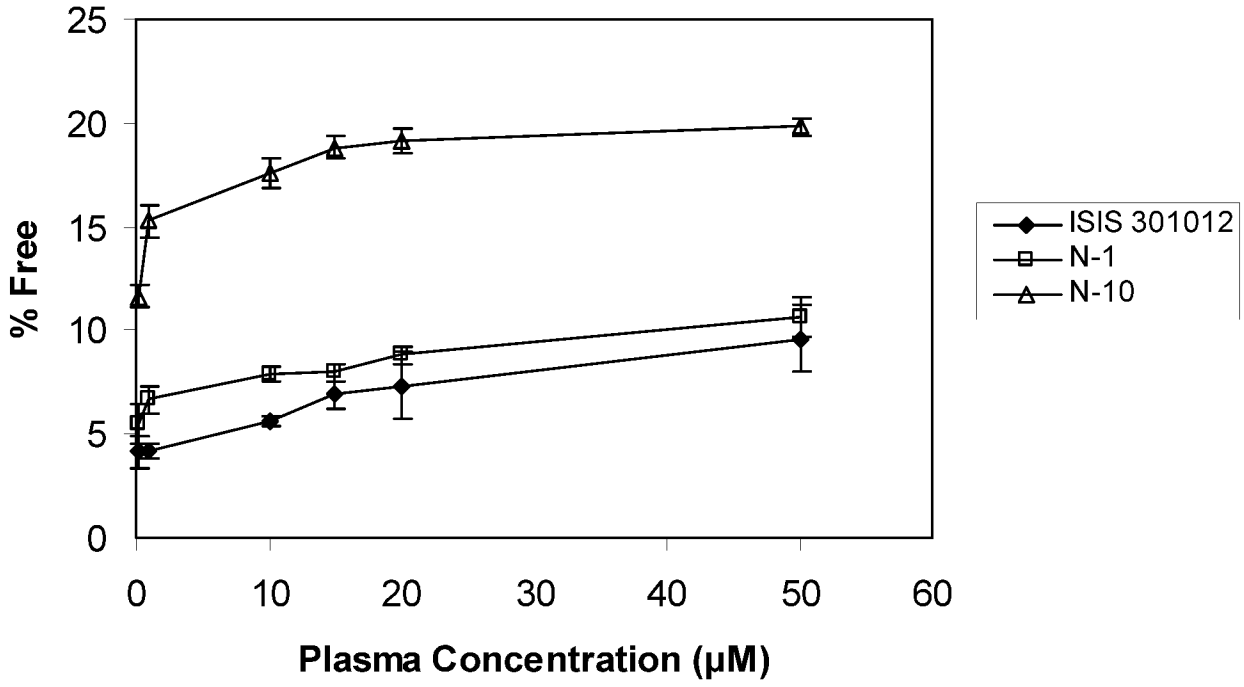

DMD Fast Forward. Published on December 15, 2006 as DOI: 10.1124/dmd.106.012401
This article has not been copyedited and formatted. The final version may differ from this version.

Figure 5

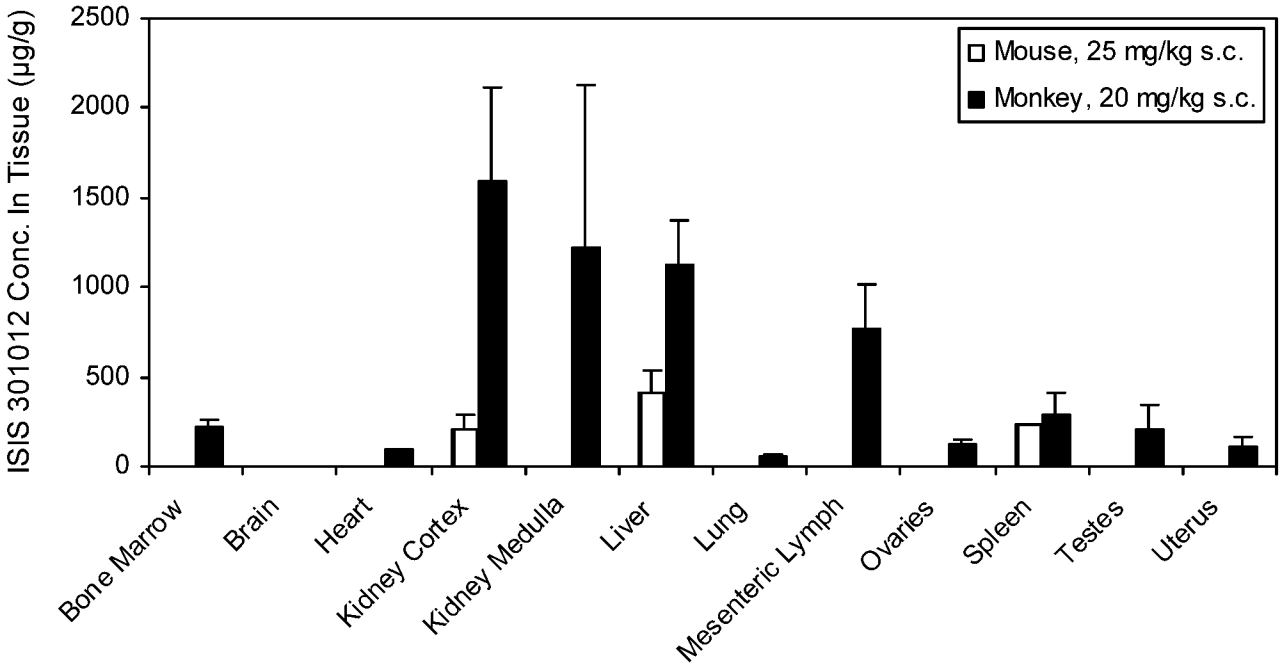

DMD Fast Forward. Published on December 15, 2006 as DOI: 10.1124/dmd.106.012401
This article has not been copyedited and formatted. The final version may differ from this version.

Figure 6a

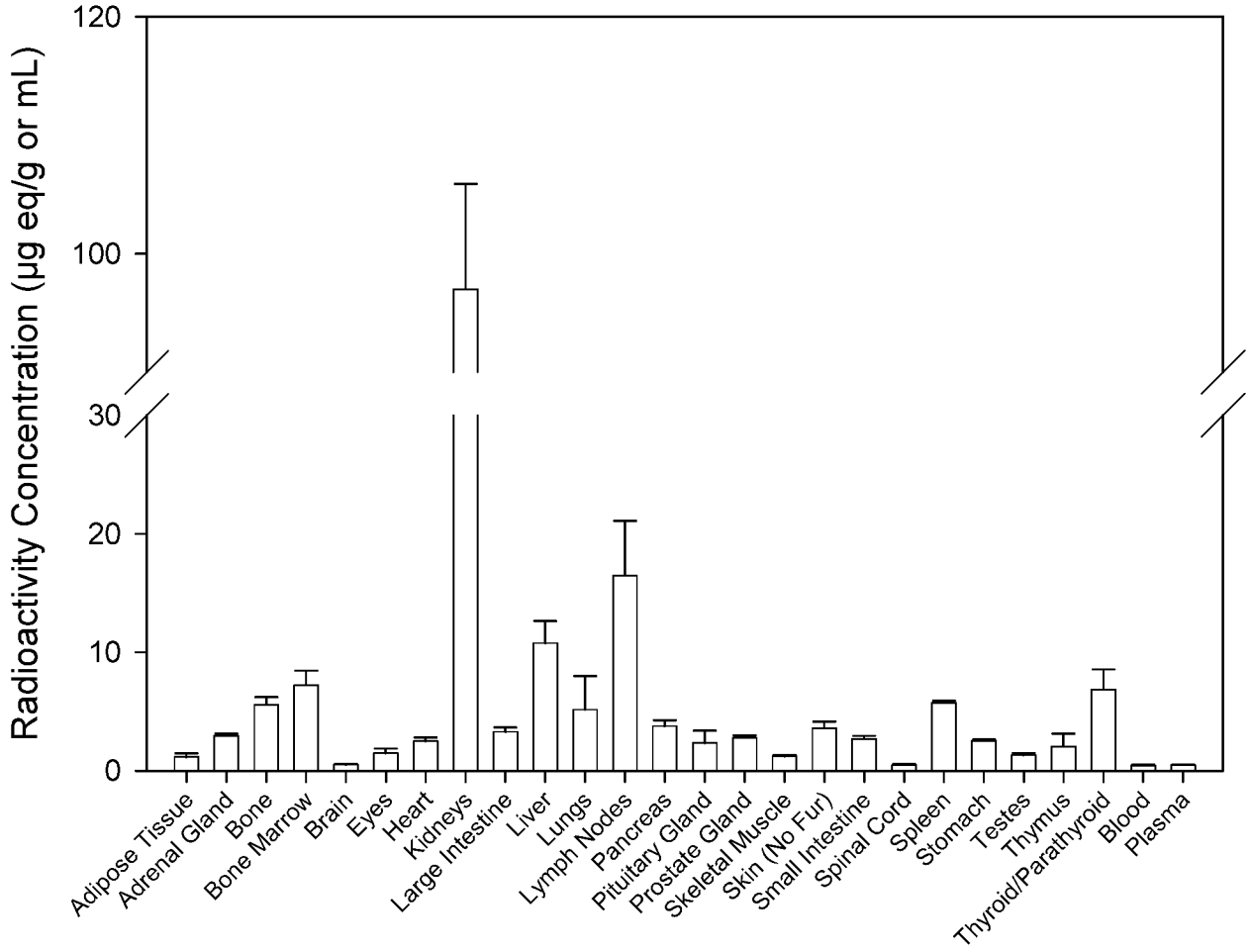

DMD Fast Forward. Published on December 15, 2006 as DOI: 10.1124/dmd.106.012401
This article has not been copyedited and formatted. The final version may differ from this version.

Figure 6b

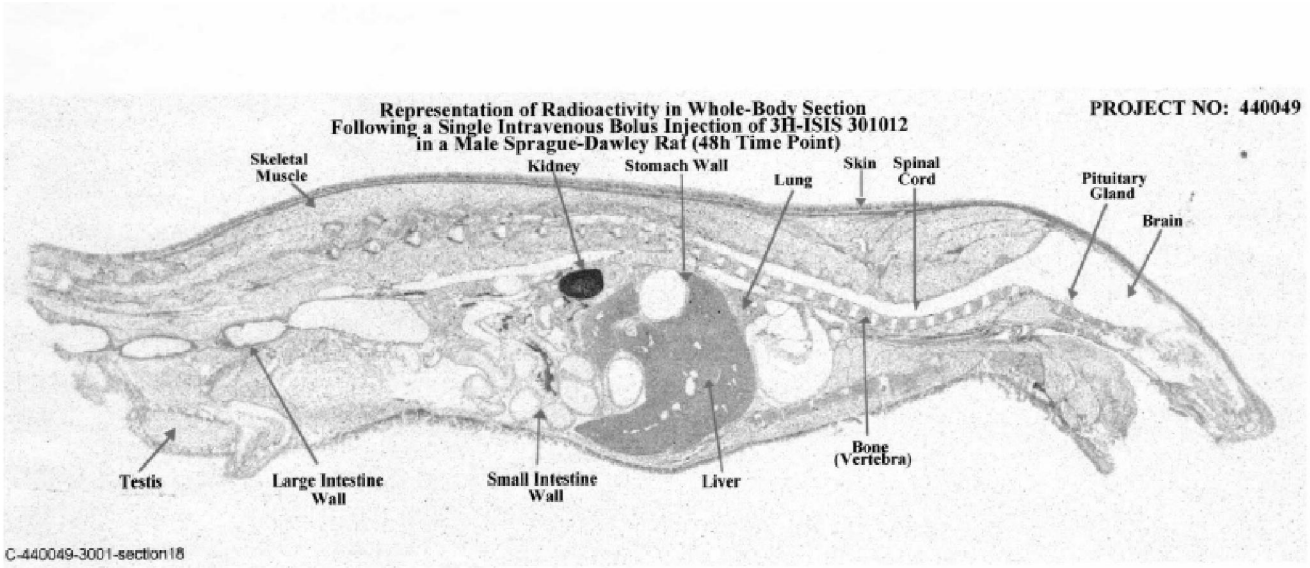

DMD Fast Forward. Published on December 15, 2006 as DOI: 10.1124/dmd.106.012401
This article has not been copyedited and formatted. The final version may differ from this version.

Figure 7

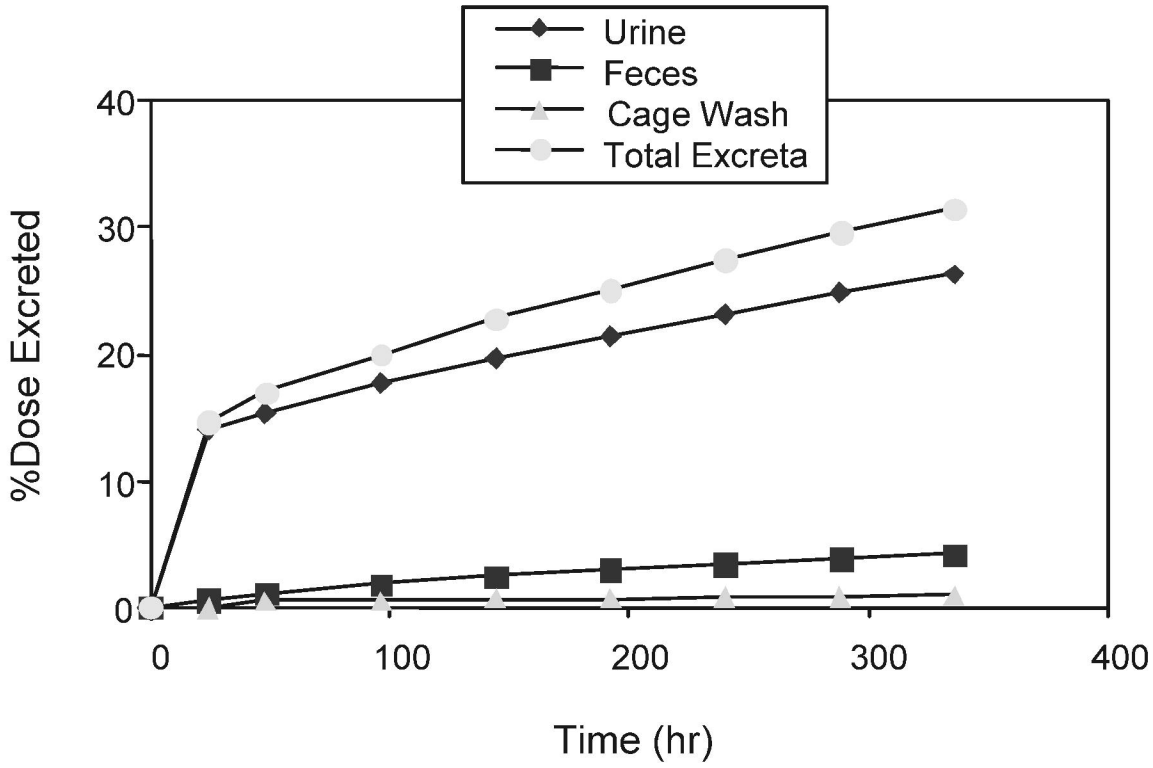

DMD Fast Forward. Published on December 15, 2006 as DOI: 10.1124/dmd.106.012401
This article has not been copyedited and formatted. The final version may differ from this version.

Figure 8

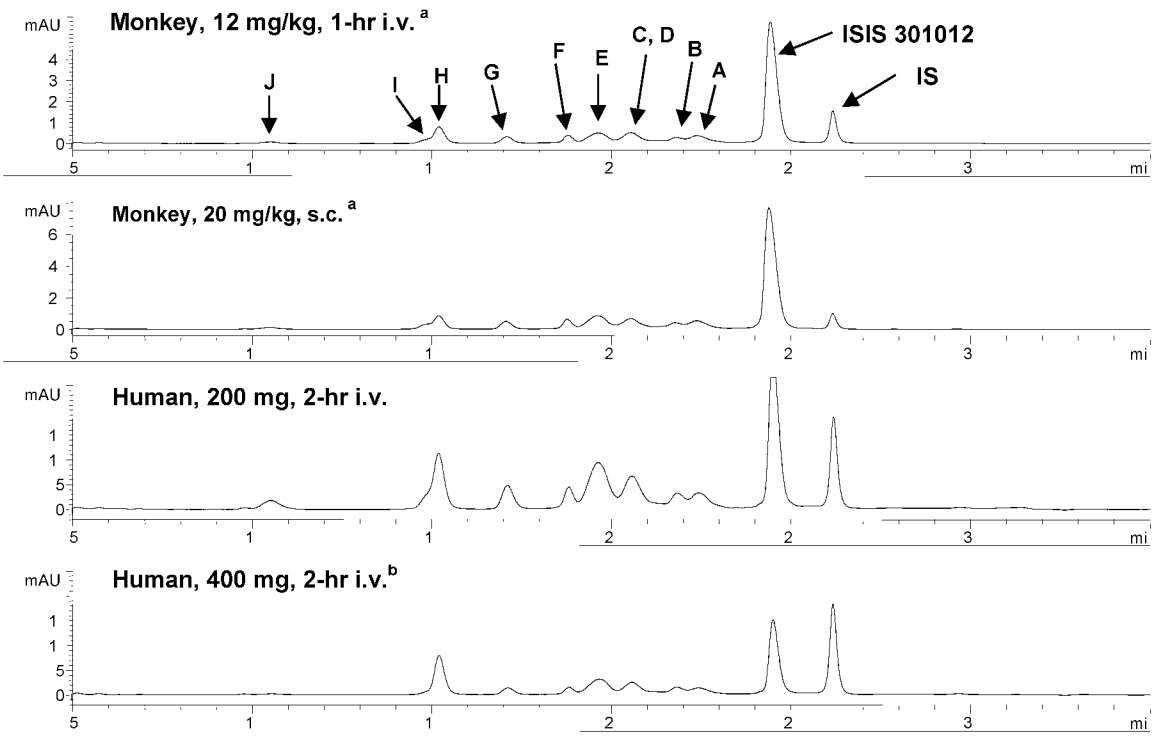

Refer to Table 3 for peak identifications.
[a] Sample was diluted 1:10 prior to extraction and analysis.
[b] Sample was diluted 1:5 prior to extraction and analysis.